

Table I—Comparison of Tensile Strength of Compacts Compressed at a Mean Force of 400 kg and the Relative Density Change Occurring during Plastic Flow and/or Crushing, ϕ

Crystal Form	Tensile Strength, kg/cm ²	ϕ
Barbital (104–152 μ m)		
Form I	2.8 \pm 0.1	0.21 \pm 0.008
Form II	2.0 \pm 0.2	0.21 \pm 0.008
Form III	3.8 \pm 0.1	0.23 \pm 0.007
Sulfathiazole (104–152 μ m)		
Form I	1.9 \pm 0.1	0.22 \pm 0.008
Form II	4.2 \pm 0.2	0.24 \pm 0.008
Aspirin (250–353 μ m)		
Form I	3.8 \pm 0.1	0.14 \pm 0.008
Form IV	8.4 \pm 0.2	0.23 \pm 0.007

between particles in the powder bed rather than the bond strength between particles. Support for this hypothesis is obtained from the data relating particle size to tensile strength of barbital Form II and sulfathiazole Form I compacts (Table II). At any mean compression force, the smaller particle-size fraction of both drugs produced the stronger compact. There will be a greater number of point contacts within compacts made from the smaller fraction and, hence, a greater area of contact between particles.

Compacts of the aspirin crystal forms also showed differences in tensile strength at a given mean compression force (Fig. 6). Tensile strength values could not be obtained for compacts of aspirin Form II because of the layering tendency of the needle-shaped crystals (6). When Form II compacts were subjected to diametral crushing, the compacts laminated.

Table II—Influence of Particle Size on the Tensile Strength of Barbital and Sulfathiazole Compacts over a Range of Mean Compression Forces

Mean Compressive Force, kg	Tensile Strength, kg/cm ² \pm 0.1			
	Barbital Form II		Sulfathiazole Form I	
	104–152 μ m	190–251 μ m	104–152 μ m	190–251 μ m
610	3.4	2.9	3.3	2.5
713	4.1	3.3	4.0	2.7
815	4.8	3.7	4.7	2.9
917	5.5	4.3	5.3	3.1

Degradation Kinetics of a Substituted Carbinolamine in Aqueous Media

H. V. MAULDING* and M. A. ZOGLIO*

Abstract □ The apparent first-order breakdown of the medicinally active agent 3-(*p*-chlorophenyl)-2-ethyl-2,3,5,6-tetrahydroimidazo[2,1-*b*]thiazol-3-ol was studied in aqueous solutions where dehydration gave the unsaturated compound 3-(*p*-chlorophenyl)-5,6-dihydro-2-ethylimidazo[2,1-*b*]thiazole. This thiazole was the primary solvolytic product produced in approximately quantitative yields for the temperature range studied and ostensibly underwent no further reaction in acidic media even on prolonged heating. Investigations were carried out at various pH values in standard buffers at constant ionic strength. The ionization constants of the compounds are reported as well as the apparent activation energies for the degradation in acid and acetate buffers. The influence of ionic

The degradation kinetics of 3-(*p*-chlorophenyl)-2-ethyl-2,3,5,6-tetrahydroimidazo[2,1-*b*]thiazol-3-ol¹ (I)

As with the polymorphic forms of sulfathiazole and barbital, there was a correlation between ϕ and the tensile strength of the compacts for aspirin Forms I and IV. The lower melting-point Form IV had the higher tensile strength at any given mean compression force, again indicating that the area of contact between particles is the overriding influence on compact strength for materials existing in different crystal forms.

REFERENCES

- (1) J. T. Fell and J. M. Newton, *J. Pharm. Pharmacol.*, **20**, 657 (1968).
- (2) J. T. Fell and J. M. Newton, *J. Pharm. Sci.*, **59**, 688 (1970).
- (3) J. M. Newton, G. Rowley, J. T. Fell, D. G. Peacock, and K. Ridgway, *J. Pharm. Pharmacol.*, **23**, 195S (1971).
- (4) D. P. Brook and K. Marshall, *J. Pharm. Sci.*, **57**, 481 (1968).
- (5) C. C. Perry and H. R. Lisner, "The Strain Gauge Primer," McGraw-Hill, London, England, 1962, p. 64.
- (6) M. P. Summers, R. P. Enever, and J. E. Carless, *J. Pharm. Pharmacol.*, **28**, 89 (1976).
- (7) J. E. Rees and E. Shotton, *ibid.*, **22**, 17S (1970).
- (8) D. Train, *ibid.*, **8**, 745 (1956).
- (9) K. Ridgway, M. Aulton, and P. H. Rosser, *ibid.*, **22**, 70S (1970).
- (10) J. E. Rees and E. Shotton, *ibid.*, **21**, 731 (1969).
- (11) M. J. Buerger, in "Phase Transformations in Solids," R. Smoluchowski, J. E. Mayer, and W. A. Weyl, Eds., Wiley, New York, N.Y., 1951, p. 183.
- (12) S. Leigh, Ph.D. thesis, London University, London, England, 1969.
- (13) M. P. Summers, Ph.D. thesis, London University, London, England, 1972.

ACKNOWLEDGMENTS AND ADDRESSES

Received June 21, 1976, from the Department of Pharmacy, Chelsea College, University of London, London, SW3 6LX, England.

Accepted for publication October 4, 1976.

M. P. Summers thanks the Science Research Council for a research studentship to allow this work to be undertaken.

* Present address: School of Pharmacy, University of London, 29/39 Brunswick Square, London, WC1N 1AX, England.

* To whom inquiries should be directed.

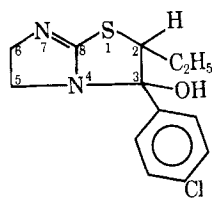
strength on the velocity constant was determined.

Keyphrases □ Thiazol-3-ol, substituted—kinetics of degradation in aqueous media, effect of temperature, pH, and ionic strength □ Degradation kinetics—substituted thiazol-3-ol, in aqueous media, effect of temperature, pH, and ionic strength □ Kinetics, degradation—substituted thiazol-3-ol, in aqueous media, effect of temperature, pH, and ionic strength □ Anorexic agents, potential—3-(*p*-chlorophenyl)-2-ethyl-2,3,5,6-tetrahydroimidazo[2,1-*b*]thiazol-3-ol, kinetics of degradation in aqueous media, effect of temperature, pH, and ionic strength

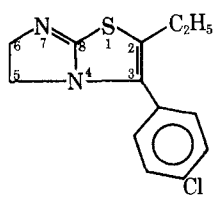
were investigated in aqueous solution at varying hydrogen-ion concentrations.

Compound I exhibits anorexic activity, and its breakdown in aqueous media is important in the formulation of

¹ No. 43976, Sandoz Pharmaceuticals, Hanover, NJ 07936.



I



II

solid and liquid dosages as well as in stability prediction of these dosage forms.

It is a somewhat unusual structural prototype in the tertiary² hydroxyl group on C-3 adjacent to N-4. These two features comprise a relatively stable carbinolamine not frequently encountered, and the structure is similar to the "pseudobases" characteristically formed from the reaction of certain quaternary heterocyclics with OH⁻ (1).

The possible existence of several isomers of I is obvious; however, X-ray crystallographic data reveal no diastereoisomerism and one conformation consisting of a *trans*-relationship between the *p*-chlorophenyl and ethyl substituents³. Kinetic evidence also rules out diastereoisomerism barring equal reaction rate constants. This finding is illustrated by the lack of deviation from a first-order plot present in parallel first-order reactions producing a common product (2).

The conversion of I to its dehydration product, 3-(*p*-chlorophenyl)-5,6-dihydro-2-ethylimidazo[2,1-*b*]thiazole⁴ (II), was the primary route of aqueous transformation of I under the conditions employed. The present work was concerned principally with this reaction.

EXPERIMENTAL

Spectrophotometric Studies in Acidic Solution—Aliquots of 10 ml of an aqueous stock solution of I hydrobromide, $2.83 \times 10^{-3} M$, were mixed with 190 ml of hydrochloric acid of the appropriate strength, previously equilibrated in a constant-temperature bath. The final concentration was $1.42 \times 10^{-4} M$ with A_{∞} of 1.760. Samples, 10 ml, were removed at various times and diluted to 20 ml with distilled water. The spectra were determined⁵ at 272 nm against blanks having the same composition but lacking I hydrobromide, $A_{\infty} = 1.760/2 = 0.880$.

Spectrophotometric Studies in Buffer Solution—Standard buffer solutions were prepared and adjusted to constant ionic strength using sodium chloride. These solutions were equilibrated in constant-temperature baths, and the same procedure was carried out as described for acidic solutions. UV spectra were determined at 272 nm using the appropriate buffers as blanks.

Determination of Ionization Constants—The hydrobromide salt of I (0.005 mole in 100 ml of water) was titrated potentiometrically with 10 equal increments of 0.1 N KOH following the method outlined by Albert and Sergeant (3). Precipitation of the base occurred before complete neutralization, but enough points were evaluated to give a pK_a of 7.60 (± 0.04).

A stock solution of II ($4.12 \times 10^{-3} M$) was prepared. The maximum difference in the absorption spectrum, at 310 nm, was obtained using 0.01 N HCl and 0.01 N NaOH solutions for the ionized and nonionized species, respectively. Aliquots of 4 ml of this solution were diluted to 200 ml with seven borate buffers, pH 8.6–9.8 and an ionic strength of less than 0.005 (4). The pK_a' value was 9.38 (± 0.04) and was verified by titration with 0.1 N KOH.

RESULTS AND DISCUSSION

With the conditions investigated, it was convenient to assay for the dehydration product, II, rather than the parent compound, I. Compound

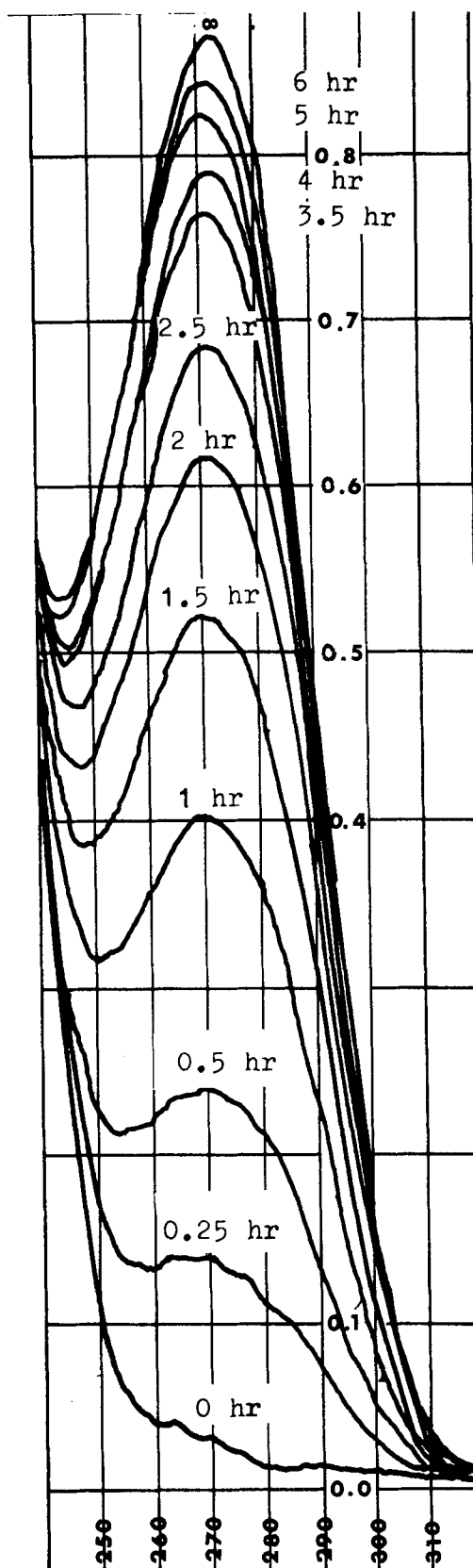


Figure 1—UV spectra for the appearance of II from I ($7.07 \times 10^{-5} M$ acetate buffer, pH 4.9, 70°, ionic strength 0.1) at various times.

II exhibited a UV absorption maximum at 272 nm which was absent in I. The molar absorptivity, a_M , was evaluated at 1.238×10^4 liters/cm mole (272 nm). Compound I exhibited an absorption maximum at 222–223 nm, $a_M = 2.55 \times 10^4$ liters/cm mole. The principal degradation route was the conversion of I to II under the conditions listed.

² It is not a tertiary carbon atom in the true sense because it is attached to two other carbons and one nitrogen.

³ Unpublished results.

⁴ No. 43978, Sandoz Pharmaceuticals, Hanover, NJ 07936.

⁵ Cary model 14 spectrophotometer.

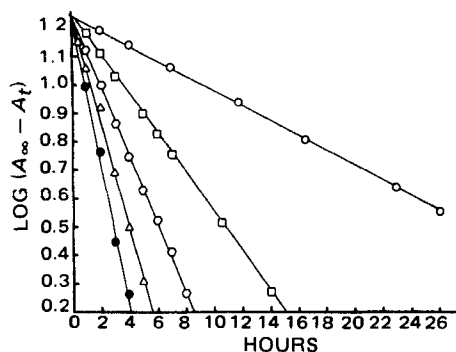


Figure 2—First-order plot for the dehydration of $7.07 \times 10^{-5} M$ I as a function of the increase in absorbance (272 nm) in hydrochloric acid at 49° . Key (hydrochloric acid concentration): \circ , 0.1 N; \square , 0.25 N; \triangle , 0.5 N; \bullet , 1.0 N.

The transformation of I to II is somewhat similar to the reported solvolysis of several cycloheximide antibiotics (5–7). However, with the cycloheximides, an equilibrium is attained between the starting material and the anhydro product.

The apparent first-order rate constants for conversion of I to II were determined using:

$$\ln(A_\infty - A_t) = -kt + \ln(A_\infty - A_0) \quad (\text{Eq. 1})$$

by which the concentration of a product of a first-order process is governed. In Eq. 1, A_∞ is the maximum absorbance, A_t is the absorbance at time t , and k is the velocity constant for the reaction.

Figure 1 illustrates the UV assay of II, with the chromophore appearing as a function of time at 272 nm. These spectra are characteristic of those obtained from pH 7 down to 2.0 N HCl and are typical of the protonated form of II, $pK_a = 9.38 (\pm 0.04)$. The positive charge, when present in both I and II, is probably located on N-7 of the amidino grouping³. The parent carbinolamine, I, showed no absorbance at 272 nm, and the previously stated analytical procedure had applicability for the interval from pH 7 to highly acid regions.

The transformation of I to II is an almost quantitative reaction. Equimolar amounts ($7.07 \times 10^{-5} M$) of I and I hydrobromide on protracted heating at several different temperatures and the previously mentioned pH's led to spectra identical to the initial spectra of II under these circumstances. Figure 1 shows a typical example where the final absorbance is 0.880 for a $7.07 \times 10^{-5} M$ solution. No further spectral change was noted on long heating at 95° .

Acid-Catalyzed Dehydration—The hydrogen-ion-catalyzed breakdown of I was carried out in 0.01–2.0 N HCl. A typical plot of these data is shown in Fig. 2 where Eq. 1 is utilized.

Figure 3 demonstrates the linear relationship of the apparent first-order velocity constants to the actual hydrogen-ion activity at several temperatures according to:

$$k = k_{H^+}[H^+] + k_0 \quad (\text{Eq. 2})$$

where $[H^+]$ was calculated from the experimental concentrations and the literature values for activity coefficients (8). The bimolecular rate constants, k_{H^+} in liters per mole hours, computed from the slopes of the lines in Fig. 3 (9–11) were: 0.24, 40° ; 0.78, 49° ; 3.20, 60° ; and 8.50, 70° . The heat of activation, ΔH_a , for the dehydration reaction was calculated by an Arrhenius plot of $\log k_{H^+}$ versus $1/T^\circ$ (absolute) for these k_{H^+} values and was 25.5 kcal/mole.

The y intercepts in Fig. 3 are equivalent to k_0 (Eq. 2) in the acidic region where $[OH^-] \sim 0$, making $k_{OH^-} [OH^-]$ approximately equal to zero (10). The extrapolated values for k_{H_2O} were: 0.25, 40° ; 0.74, 49° ; 2.2, 60° ; and 5.8, 70° ; with a resultant heat of activation of 22.5 kcal/mole.

Ionic Strength Influence—In the dehydration of a molecule containing a positive center such as I, primary kinetic salt effects may be anticipated. Perturbation of the reaction rate constant on addition of neutral salts is to be expected from the Bronsted-Bjerrum equation (12):

$$\log k = \log k_0 + 1.02Z_A Z_B \sqrt{\mu} \quad (\text{Eq. 3})$$

Equation 3 may be applied to reactions between ionic species where k_0 is the rate constant in an infinitely dilute solution, Z_A and Z_B are the charges on reactants A and B, and μ is the ionic strength. From this expression, a positive salt effect should occur in a hydronium-ion-catalyzed

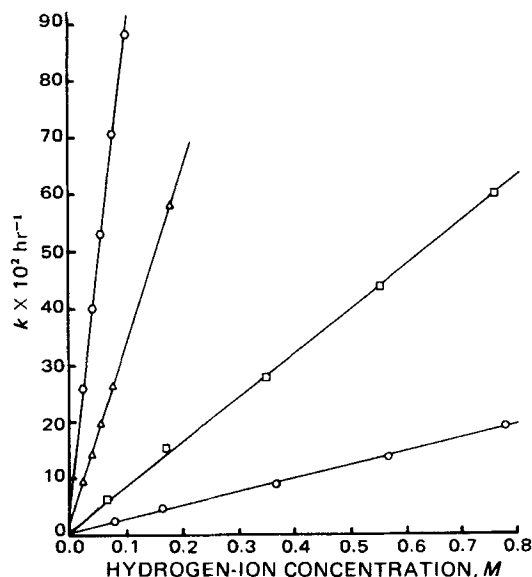


Figure 3—Rate constants, k , in hr^{-1} for the apparent first-order degradation of I as a function of the hydrogen-ion activity, $[H^+]$, at 70° (\circ), 60° (\triangle), 49° (\square), and 40° (\diamond).

dehydration of I and a negative effect should occur where the reaction is catalyzed by negative ions, i.e., hydroxide and acetate. These salt effects should be evident at pH values below 5.5 [pK_a of I = $7.60 (\pm 0.04)$] where I is 99% in the cationic form.

Unfortunately, the equation only holds for extremely dilute solutions, $\mu = 0.01$ or less, of 1:1 electrolytes. Although the relationship has no theoretical justification at higher ionic strengths (13), qualitative agreement may be seen in many cases with both positive and negative deviations as predicted (14–16).

Breakdown of I with a loss of water to give II was carried out in 0.05 N HCl made to final ionic strengths with sodium chloride. The temperature was 70° ; UV analysis was performed at 272 nm. Figure 4 illustrates the linear relationship obtained when the log apparent first-order velocity constants were plotted versus the square root of the ionic strength. The same straight-line relationship is shown in Fig. 5 describing the dehydration of I at 40° in pH 4.48 acetate buffer (0.1 M CH_3COONa) with sodium chloride added to increase the ionic strength.

The equation predicts a slope of 1.02 under proper conditions, but Figs. 4 and 5 show that a slope of considerably less than one was obtained in both cases. These results give information concerning the primary salt effects. A linear dependence of $\log k$ versus $\sqrt{\mu}$ was seen throughout the ranges of ionic strength studied, with the expected slope signs positive for hydronium-ion-catalyzed breakdown (Fig. 4) and negative for hydroxide- and acetate-catalyzed degradation (Fig. 5). The positive slope of Fig. 4 indicates two positive ions in the transition state, while the negative slope of Fig. 5 indicates a positive and a negative charge according to the Bronsted equation.

pKa Determinations—Compound II offered no significant difficulties in the evaluation of its ionization constant because the ionized and nonionized species exhibited considerable differences in absorbance at 310 nm. The pK_a of 9.38 (± 0.04) was determined spectrophotometrically

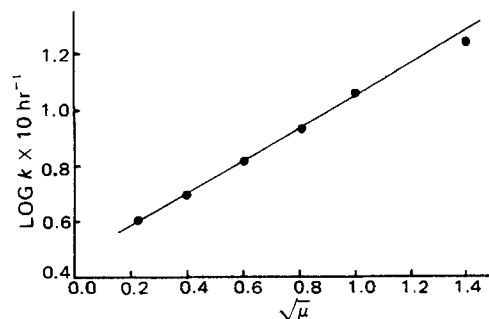


Figure 4—Effect of ionic strength on the rate of hydronium-ion-catalyzed degradation of I at 70° in 0.05 N HCl. Sodium chloride was added as the neutral salt to increase ionic strength.

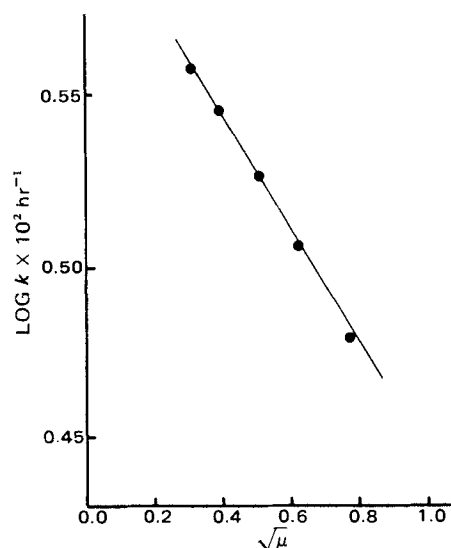


Figure 5—Effect of ionic strength on the rate of dehydration of I at 40°, pH 4.48, and 0.1 M sodium acetate. Sodium chloride was added to increase ionic strength.

in the usual manner (4) by UV readings in a series of borate buffers and was corroborated by titration.

Compound I posed a problem in the absence of an easily usable UV spectrum and precipitation of the free base on attempted titration of the hydrobromide salt by potassium hydroxide (3). The more difficult solubility procedure (4) could not be easily applied in this situation due to complications arising from the conversion of I to II in the buffers needed for the studies.

A modification of the titration method was adapted using:

$$\text{pKa} = \text{pH} + \log \frac{\text{BH}^+}{\text{B}} \quad (\text{Eq. 4})$$

where $\text{BH}^+ = \text{I}$ hydrobromide and $\text{B} = \text{I}$ (free base), both in concentration terms. Previously, good results were attained by partial titration, even in instances of free base precipitation (17). The pKa values were calculated for the interval $\log (\text{BH}^+/\text{B}) = 49/1$ to $9/1$. No precipitation of base was noted in this range, and the pKa value obtained was 7.60 (± 0.04).

Degradation in Buffers—Tables I and II list the observed first-order rate constants obtained in formate and acetate buffers, pH 3–5, under the experimental conditions. Figure 6 shows the observed rate constants (Tables I and II) for formate buffer, pH 4.1, 70°, and acetate buffer, pH 4.1, 60 and 70°, plotted against acetate- and formate-ion concentrations. This plot constitutes the usual test for general base catalysis (10). The data points are not aligned in the predicted linear manner but curve rather sharply downward at low buffer concentrations. The same situation is noted in Fig. 8, where acetate concentration ranged between 0.003 and 0.200 M.

This somewhat unusual phenomenon was encountered (18) in the sulfur to nitrogen acetyl transfer reaction of *S*-acetyl- β -mercaptoeth-

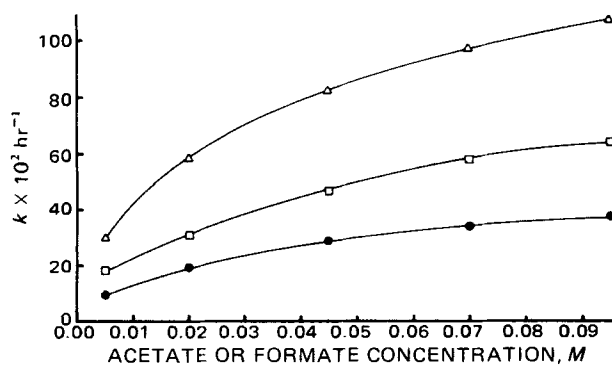


Figure 6—Plot of the observed first-order rate constants for dehydration of I in $k \times 10^2 \text{ hr}^{-1}$ as a function of acetate or formate concentration. Ionic strength was constant at 0.10, and the pH was 4.1. Key: Δ , acetate at 70°; \bullet , acetate at 60°; and \square , formate at 70°.

Table I—Observed First-Order Rate Constants^a (k , hr^{-1}) for Dehydration of $7.07 \times 10^{-5} \text{ M I}$ in Formate Buffer at 70°^b

pH	Formate Ion, M	k , hr^{-1}
3.0	0.005	0.20
	0.020	0.32
	0.070	0.59
3.5	0.005	0.20
	0.020	0.31
	0.048	0.49
	0.070	0.56
	0.095	0.69
4.1	0.005	0.18
	0.020	0.31
	0.045	0.46
	0.070	0.58
	0.095	0.64

^a Based on UV absorbance data for formation of unsaturated product (Eq. 1).

^b The pH values were read at the indicated temperature on a pH meter standardized at the temperature. Ionic strength was made up to 0.1 with sodium chloride in all solutions.

ylamine and was described as a two-step mechanism with a rate-limiting buffer-catalyzed step. The reaction rate rises sharply at low acetate- and formate-ion concentrations followed by an uncatalyzed rate-limiting step at high buffer concentrations. This nonlinear dependence of the rate constants on acetate and formate concentration is characterized by a considerable decrease in slope at relatively high buffer concentrations.

In the $\text{I} \rightarrow \text{II}$ transformation, a similar two-step process occurs with a relatively large catalytic constant at low acetate or formate concentrations and a smaller constant at higher acetate or formate concentrations. Barnett and Jencks (19) further clarified this mechanism by dissecting the data into appropriate rate constants through computerization and standard techniques.

Tables I and II show the rate constants to be relatively independent of pH for the acetate (pH 4–5) and formate (pH 3–4) systems, which is in agreement with previous work (18, 19).

Arrhenius plots for the decomposition of I in pH 4.1 acetate buffer (Table II) are shown in Fig. 7. The apparent energies of activation ranged between 24 and 25.5 kcal/mole for the various acetate concentrations.

Table II—Observed First-Order Rate Constants^a (k , hr^{-1}) and Experimental Conditions for Dehydration of $7.07 \times 10^{-5} \text{ M I}$ in Acetate Buffer Solution

pH ^b	Acetate Ion, M	Ionic Strength ^c	k , hr^{-1}		
			40°	60°	70°
4.1	0.005	0.10	0.0075	0.0962	0.29
	0.020		0.0181	0.1994	0.58
	0.045		0.0265	0.2887	0.82
	0.070		0.0327	0.3408	0.96
	0.095		0.0359	0.3794	1.08
4.5	0.005	0.10	—	0.0984	0.30
	0.020		—	0.2101	0.61
	0.045		—	0.2986	0.86
	0.070		—	0.3569	1.00
	0.095		—	0.3658	1.09
5.0	0.005	0.10	0.0112	0.1006	0.31
	0.020		0.0209	0.2094	0.60
	0.045		0.0166	0.2951	0.89
	0.070		0.0310	0.3583	1.00
	0.095		0.0351	0.3755	1.07
4.1	0.015	0.20	—	—	0.48
	0.045		—	—	0.82
4.5	0.015	0.20	—	0.1598	0.50
	0.045		—	0.2725	0.81
	0.095		—	0.3522	—
	0.145		—	0.3906	—
	0.195		—	0.4120	—
5.0	0.015	0.20	—	0.2071	0.51
	0.045		—	0.2910	0.85
	0.095		—	0.4173	—
	0.145		—	0.4407	—
	0.195		—	0.4998	—

^a See Table I. ^b See Table I. ^c Sodium chloride was added to produce proper ionic strength.

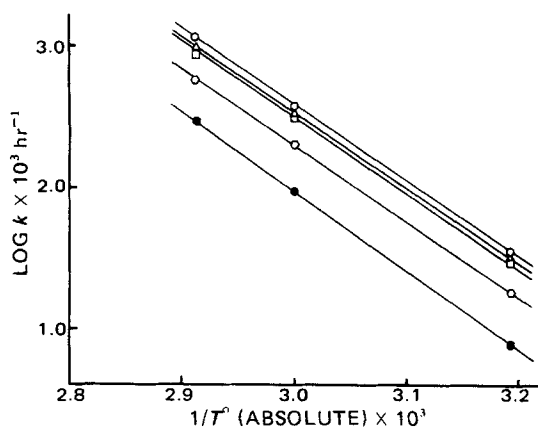


Figure 7—Typical Arrhenius plots for degradation of I in pH 4.1 acetate buffer (Table II) at various acetate-ion concentrations. Key (acetate concentration): ●, 0.005 M; ○, 0.020 M; □, 0.045 M; △, 0.070 M; and ○, 0.095 M.

Concentrations of acetate below 3×10^{-3} M (Fig. 8) could not be employed with the pH maintained constant, thus preventing studies at lower acetate-ion concentrations. The results in Fig. 8 should theoretically extrapolate at zero buffer concentration to the k_0 value (Eq. 2). Examination of k_0 for the acetate system in Fig. 8 shows that of its three components, k_{H_2O} , $k_{H^+}[H^+]$, and $k_{OH^-}[OH^-]$, the first has a predominant importance, $k_{H_2O} = 2.2$, 60° . The reasoning is that the $[H^+]$ of 3×10^{-5} M, pH 4.5, multiplied by $k_{H^+} = 3.2$, 60° , provides a negligible contribution, while k_{OH^-} seems to play a relatively unimportant role due to the small effect noted on the rate constants in the pH 4–5 range.

The values in Table II for the various pH values at a given temperature are almost within the limits of experimental error. Thus, it appears that the value for k_0 (Fig. 8) should be somewhat above the value of 2.2 hr^{-1} for k_{H_2O} at 60° . Figure 6 shows that the y intercept for formate and acetate ions at 70° also might be extrapolated to approximately the k_{H_2O} value at that temperature. This nonlinear dependency of the data upon anionic concentrations may be noted in all results listed in Tables I and II.

Notari *et al.* (20) reported a similar phenomenon taking place in a deamination reaction, except that the acidic buffer component exerted the principal catalytic effect.

These results are indicative of a reaction rate constant plateau in the pH range of 3–5 with little OH^- or H^+ effect. The primary route of breakdown is water attack on the protonated form of I. In this pH 3–5 region, general bases catalyze in what may be a two-step sequence (18–20).

Preliminary investigations with phosphate buffers demonstrate this

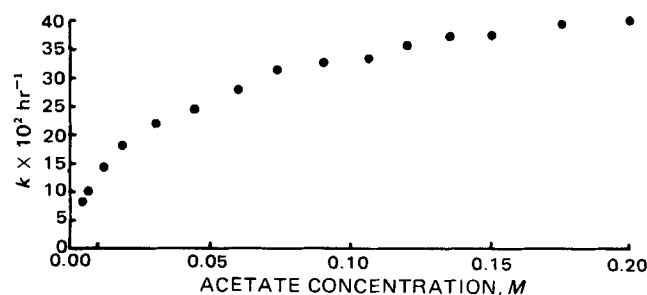


Figure 8—Plot of the observed first-order rate constant for dehydration of I versus acetate concentration at 60° , pH 4.5, with ionic strength maintained with sodium chloride. The pH values were measured at 60° on a pH meter standardized at that temperature and were within 0.04 of the stated value of 4.5. Rate constants were reproducible within 5%. Ionic strength was constant at 0.20. These data are not listed in Table II.

nonlinear dependency at pH 5.7 as was found with the acetate systems. However, at higher pH values (6.0 and 6.7), typical linear data were encountered (Table III). Studies were not carried out above pH 6.7 due to the insolubility of the basic form of I, pK_a 7.6.

SUMMARY

Compound I undergoes apparent first-order degradation under the conditions examined, producing the dehydration product II in almost quantitative yields.

Elimination of the C-2 hydrogen and the C-3 hydroxyl substituents of I takes place in aqueous solution since their *trans*-conformational relationship tends to facilitate this reaction.

The mechanism of acid-catalyzed dehydration probably involves protonation of the hydroxyl group followed by formation of a carbonium ion and elimination of a proton to produce the dehydro product. Conversely, base catalysis is initiated by removal of a proton followed by elimination of an OH^- . These well-known processes were discussed for streptovitacin A dehydration (7).

Observed rate constants did not show the usual linear dependency in acetic acid–acetate buffers. Curves were obtained with negative deviation from linearity. This result was probably due to a change in the rate-determining step.

The observed rate constant for this transformation in the absence of other species (e.g., buffers and salts) may be written to pH 5 as $k = k_{H^+}[H^+] + k_{H_2O}$ with actual data closely following calculated values. Water attack on the protonated substrate occurred and seemed to be the principal cause of degradation in the pH 3–5 range. The molecule exhibited greatest stability in this region, but degradation was accelerated considerably by addition of general bases.

The compound shows rather pronounced salt effects, both positive and negative, depending on the reaction conditions.

REFERENCES

- (1) D. Magrath and J. Phillips, *J. Chem. Soc.*, **1949**, 1940.
- (2) H. C. Brown and R. S. Fletcher, *J. Am. Chem. Soc.*, **71**, 1845 (1949).
- (3) A. Albert and E. P. Sergeant, "Ionization Constants of Acids and Bases," Wiley, New York, N.Y., 1962, pp. 16–42.
- (4) *Ibid.*, pp. 69–91.
- (5) E. R. Garrett and R. E. Notari, *J. Org. Chem.*, **31**, 425 (1966).
- (6) E. R. Garrett and R. E. Notari, *J. Pharm. Sci.*, **54**, 209 (1965).
- (7) R. E. Notari and S. M. Caiola, *ibid.*, **58**, 1203 (1969).
- (8) H. S. Harned and R. B. Owen, "The Physical Chemistry of Electrolytic Solutions," 3rd ed., Reinhold, New York, N.Y., 1958.
- (9) E. R. Garrett, *J. Am. Chem. Soc.*, **82**, 827 (1960).
- (10) E. R. Garrett, *J. Pharm. Sci.*, **51**, 811 (1962).
- (11) E. R. Garrett, "Advances in Pharmaceutical Sciences," vol. 2, Academic, New York, N.Y., 1967, p. 1.
- (12) S. Glasstone, K. J. Laidler, and H. Eyring, "The Theory of Rate Processes," McGraw-Hill, New York, N.Y., 1941, p. 427.
- (13) A. G. Frost and R. G. Pearson, "Kinetics and Mechanism," 2nd ed., Wiley, New York, N.Y., 1965, p. 151.
- (14) S. Siegel, L. Lachman, and L. Malspeis, *J. Am. Pharm. Assoc.*,

Table III—Observed First-Order Rate Constants^a (k , hr^{-1}) for Dehydration of 7.07×10^{-5} M I in Phosphate Buffer at 60° ^b

pH ^c	Buffer Composition, M ^d		k , hr^{-1}
	Monobasic Sodium Phosphate Monohydrate	Dibasic Sodium Phosphate Heptahydrate	
5.70 ± 0.04	0.150	0.015	0.42
	0.110	0.011	0.39
	0.070	0.007	0.33
	0.030	0.003	0.26
6.00 ± 0.05	0.115	0.0283	0.54
	0.0805	0.0198	0.50
	0.0575	0.0142	0.47
	0.046	0.0113	0.45
6.70 ± 0.04	0.023	0.0057	0.42
	0.050	0.050	0.64
	0.035	0.035	0.60
	0.030	0.030	0.57
	0.020	0.020	0.52
	0.005	0.005	0.44

^a See Table I. ^b See Table I. ^c The pH values were read at the indicated temperatures before, during, and after a run. ^d Stock solutions were diluted to give indicated strengths followed by addition of sodium chloride to obtain an ionic strength of 0.2.

Sci. Ed., 48, 431 (1959).

- (15) R. B. Bell and F. J. Lindlars, *J. Chem. Soc.*, 1954, 4601.
(16) E. R. Garrett, *J. Am. Chem. Soc.*, 79, 5206 (1957).
(17) H. V. Maulding and M. A. Zoglio, *J. Pharm. Sci.*, 59, 700 (1970).
(18) R. B. Martin, R. I. Heddrick, and A. Parcell, *J. Org. Chem.*, 29, 3197 (1964).
(19) R. E. Barnett and W. P. Jencks, *J. Am. Chem. Soc.*, 91, 2358 (1969).
(20) R. E. Notari, M. L. Chin, and A. Cardoni, *J. Pharm. Sci.*, 59, 28 (1970).

ACKNOWLEDGMENTS AND ADDRESSES

Received February 9, 1970, from the *Pharmacy Research and Development Department, Sandoz Pharmaceuticals, Hanover, NJ 07936.*

Accepted for publication April 8, 1970. (Publication delayed at request of authors.)

The authors acknowledge the technical assistance of Miss Virginia Nieman.

* Present address: Merrell-National Laboratories, Cincinnati, OH 45215.

* To whom inquiries should be directed.

Quantification of Lidocaine and Several Metabolites Utilizing Chemical-Ionization Mass Spectrometry and Stable Isotope Labeling

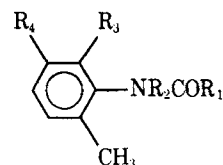
S. D. NELSON, W. A. GARLAND, G. D. BRECK, and W. F. TRAGER*

Abstract □ Quantification of the suspected metabolites of lidocaine in humans was carried out using the direct insertion probe and chemical-ionization mass spectrometry. Deuterated analogs of the metabolites of lidocaine were added to serial human plasma and urine samples and were used as internal standards following oral administration of 250 mg of lidocaine hydrochloride monohydrate to two male subjects and 202 mg of lidocaine free base to one male subject. The average results after analysis of the 0–24-hr urine samples, before β -glucuronidase-sulfatase treatment, indicated the presence of seven of the possible metabolites in the following amounts (percent of administered dose based on the free base): lidocaine, 1.95; ω -ethylamino-2,6-dimethylacetanilide, 4.90; ω -amino-2,6-dimethylacetanilide, 0.88; *m*- and/or *p*-hydroxylidocaine, 0.73; *m*- and/or *p*-hydroxy- ω -ethylamino-2,6-dimethylacetanilide, 0.56; 2,6-dimethylaniline, 0.97; and 4-hydroxy-2,6-dimethylaniline, 63.5. Both *N*-ethyl- and *N,N*-diethylglycine were detected in human and Rhesus monkey urine, although quantification was not achieved.

Keyphrases □ Lidocaine and various metabolites—chemical-ionization mass spectrometric and stable isotope labeling analyses, human plasma and urine □ Chemical-ionization mass spectrometry—analyses, lidocaine and various metabolites, human plasma and urine □ Stable isotope labeling—analyses, lidocaine and various metabolites, human plasma and urine □ Anesthetics, local—lidocaine and various metabolites, chemical-ionization mass spectrometric and stable isotope labeling analyses, human plasma and urine

Lidocaine (*Ia*) is a widely used local anesthetic and antiarrhythmic agent. At present, it is generally considered the most useful drug in suppressing ventricular arrhythmias, which occur in approximately 80% of all myocardial infarction cases (1–3). Based on the structure of the drug, three sites are susceptible to metabolic attack: the tertiary amino group, the amide linkage, and the aromatic ring. The tertiary amino group is susceptible to *N*-oxidation and oxidative *N*-dealkylation (4). The amide linkage is susceptible to hydrolysis by microsomal amidases (5) and to oxidation by liver microsomes to an *N*-hydroxyamide (4). The aromatic ring and the aryl methyl groups are also susceptible to hydroxylation (4). Many of these reactions were detected using nonspecific colorimetric assays and paper chromatography (6–9) and, more recently, more specific GC methods (10–12).

Using electron-impact mass spectrometry, Breck and Trager (13) confirmed the presence of lidocaine, ω -ethylamino-2,6-dimethylacetanilide (*Ib*), and 2,6-dimethylaniline (*Ia*) in human urine following an oral dose or an intravenous infusion of lidocaine. They also detected small amounts of a new cyclic metabolite of lidocaine, *N*¹-ethyl-2-methyl-*N*³-(2,6-dimethylphenyl)-4-imidazolidinone (*III*). GC-mass spectrometry was used to detect and quantify lidocaine and its two *N*-deethylated metabolites, *Ib* and ω -amino-2,6-dimethylacetanilide (*Ic*), in the plasma and urine of patients receiving intravenous infusions of the drug for the treatment of cardiac arrhythmias (14, 15). Under these conditions, lidocaine levels ranged from 1.2 to 15 μ g/ml, *Ib* levels ranged from 0.2 to 2.4 μ g/ml, and *Ic* levels ranged from <1.0 to 2.7 μ g/ml, with



- Ia*: R₁ = CH₂N(CH₂CH₃)₂, R₂ = H, R₃ = CH₃, R₄ = H
*Ia-d*₄: R₁ = CH₂N(CD₂CH₃)₂
Ib: R₁ = CH₂NHCH₂CH₃, R₂ = H, R₃ = CH₃, R₄ = H
*Ib-d*₃: R₁ = CH₂NHCH₂CD₃
Ic: R₁ = CH₂NH₂, R₂ = H, R₃ = CH₃, R₄ = H
*Ic-d*₂: R₁ = CD₂NH₂
Id: R₁ = CH₂N(CH₂CH₃)₂, R₂ = H, R₃ = CH₃, R₄ = OH
*Id-d*₄: R₁ = CH₂N(CD₂CH₃)₂
Ie: R₁ = CH₂NHCH₂CH₃, R₂ = H, R₃ = CH₃, R₄ = OH
*Ie-d*₃: R₁ = CH₂NHCH₂CD₃
If: R₁ = CH₂N(CH₂CH₃)₂, R₂ = H, R₃ = CH₂OH, R₄ = H
Ig: R₁ = CH₂NHCH₂CH₃, R₂ = H, R₃ = CH₂OH, R₄ = H
*Ig-d*₂: R₂ = CD₂OH
Ih: R₁ = CH₂N(CH₂CH₃)₂, R₂ = OH, R₃ = CH₃, R₄ = H
*Ih-d*₄: R₁ = CH₂N(CD₂CH₃)₂
Ii: R₁ = CH₂NHCH₂CH₃, R₂ = OH, R₃ = CH₃, R₄ = H
*Ii-d*₃: R₁ = CH₂NHCH₂CD₃
Ij: R₁ = CH₂N(CH₂CH₃)₂, R₂ = H, R₃ = CH₃, R₄ = H
O